

Moments of the Proton F_2 Structure Function at Low Q^2

C.S. Armstrong,¹ R. Ent,¹ C.E. Keppel,^{1,2} S. Liuti,^{3,4} G. Niculescu,⁵ I. Niculescu^{1,6}

¹ Thomas Jefferson National Accelerator Facility, Newport News, Virginia 23606 ² Hampton University, Hampton, Virginia 23668 ³ University of Virginia, Charlottesville, Virginia 22901 ⁴ INFN Sezione di Roma Tre, Roma, Italy ⁵ Ohio University, Athens, Ohio 45701 ⁶ The George Washington University, Washington, D.C. 20052

(November 2, 2018)

We investigate the Q^2 dependence of inclusive electron-proton scattering F_2 structure function data in both the nucleon resonance region and the deep inelastic region, at momentum transfers below 5 (GeV/c)^2 . From these data we construct moments of F_2 , down to momentum transfers of $Q^2 \approx 0.1 \text{ (GeV/c)}^2$. The second moment is only slowly varying with Q^2 down to $Q^2 \approx 1 \text{ (GeV/c)}^2$, which is a reflection of duality. Below Q^2 of 1 (GeV/c)^2 , the Q^2 dependence of the moments is predominantly governed by the elastic contribution, whereas the inelastic channels still seem governed by local duality.

I. INTRODUCTION

Perturbative QCD (pQCD) describes the scale dependence of a wide number of hard processes, up to Next to Leading Order (NLO), and in a few cases up to Next to Next to Leading Order (NNLO) [1]. However, direct comparisons of calculations with experimental cross sections are often affected by the uncertainty coming from non-perturbative contributions, that are less well understood, although exceptional cases exist where the non-perturbative corrections can be deduced from the large distance behavior of the perturbative series [2]. To this date, the mechanisms by which a pQCD description of deep inelastic observables starts failing, giving way to non-perturbative (NP) behavior, are still largely undetermined. New studies of kinematic regions, and possible observables expected to be most sensitive to this transition, are currently being pursued.

This paper is dedicated to interpreting a somewhat surprising behavior of the nucleon structure function F_2 in the nucleon resonance region, as recently measured at Jefferson Lab and reported in [3,4], for four-momentum transfers squared $0.45 \leq Q^2 \leq 3.3 \text{ (GeV/c)}^2$. This behavior is consistent with older, lower precision, SLAC data, down to $Q^2 = 0.07 \text{ (GeV/c)}^2$ [5]. At the lower values of Q^2 , the resonance region, typically defined to comprise the region in invariant mass $M^2 < W^2 (= M^2 + Q^2(1/x - 1)) < 4 \text{ GeV}^2$, with M the proton mass and x the Bjorken scaling variable, is at low values of x , $x \approx 0.1$. Thus, the resonances do not characterize the large x behavior that was extensively studied before, in e.g. Refs. [6–9]. It was, however, found that the resonance region seems to

average to a single curve even at these very low values of Q^2 . This scaling curve mimics a valence-like quark distribution, the new data of [3] adding new information for $x \leq 0.25$.

It is the aim of this paper to present a low- Q^2 moment analysis of the inclusive electron-proton scattering F_2 structure function data, based upon the new precise resonance region and existing deep inelastic region data, and to interpret these moments in the context of the surprising resonance region behavior of [3]. Such an analysis would extend previous pQCD analyses of the type performed in [10,6–9], to the lowest values of Q^2 and x of [3]. In particular, as Q^2 decreases, we expect NP effects to dominate the cross section, reducing the agreement with pQCD predictions. Such an analysis may be complementary to the ones addressing another set of low- Q^2 measurements of F_2 obtained recently at HERA [11], which however belong to a completely different kinematical region, characterized by very low x (down to $x \approx 10^{-6}$) and, accordingly, to very large W^2 . In [11] it has been found that the structure function F_2 can be described by pQCD down to $Q^2 \approx 1 \text{ (GeV/c)}^2$, provided a gluon distribution vanishing at low x (also referred to in the literature as “valence-like” [11]) and a non vanishing but small sea distribution, are adopted. However, in Ref. [11] it was also found that, at even lower values of Q^2 , $0.045 \leq Q^2 \leq 0.65 \text{ (GeV/c)}^2$, and in the same very low x region, the pQCD description breaks down giving way to different types (*e.g.* Regge type) of descriptions.

The fact that pQCD can be extended to very low Q^2 ($Q^2 \approx 1 \text{ (GeV/c)}^2$) was unexpected and supports the idea that the QCD coupling constant might have a smoother behavior at low Q^2 than predicted by asymptotic freedom expressions. Or, in other words, the confinement mechanism might manifest itself in a softer way [12–14]. It is also unexpected from the point of view of a pQCD based analysis that the resonance data, lying on the low side of the invariant mass spectrum, would follow a curve that is not too far from the DIS valence quark curve down to very low Q^2 . Is this still a signature of pQCD?

In Section II we remind the reader of the Bloom-Gilman duality phenomenon. In Section III we review the world inclusive (e, e') data at low Q^2 , both in the low and in the large W^2 regions. In Section IV, we evaluate the moments of the proton structure function in the low Q^2 region, including the elastic contribution, and we extend the pQCD based analysis of [9] to this region. In

Section V, we discuss the role played by the elastic contribution in rendering the Q^2 dependence of the moments. In Section VI, we draw our conclusions.

II. BLOOM-GILMAN DUALITY

Three decades ago, Bloom and Gilman observed a fascinating correspondence between the resonance electroproduction and deep inelastic kinematic regimes of inclusive electron-nucleon scattering [15]. Specifically, it was observed that the resonance strength could be related to the deep inelastic strength via a scaling variable which allowed for a comparison of the lower W^2 and Q^2 resonance region data to the higher W^2 and Q^2 deep inelastic data. It was observed that the deep inelastic data are apparently equivalent to an average of the resonance region data. Furthermore, this behavior was observed over a range in Q^2 and W^2 , and it was found that, with changing Q^2 , the resonances move along, but always average to, the smooth scaling curve typically associated with deep inelastic scattering (DIS). This behavior clearly hinted at a common origin for resonance (hadron) electroproduction and deep inelastic (partonic) scattering, termed parton-hadron, or Bloom-Gilman, duality.

A global kind of parton-hadron duality is well established: low-energy resonance production can be shown to be related to the high-energy behavior of hadron-hadron scattering [16–18]; the familiar ratio of $e^+e^- \rightarrow$ hadrons over $e^+e^- \rightarrow$ muons uses duality to relate the hadron production to the sum of the squared charges of the quarks: here duality is guaranteed by unitarity (in this, one could argue that the ρ production channel exhibits local duality, in that its area averages to about the same global value) [19]; in pQCD the high-momentum transfer behavior of nucleon resonances can be related to the high-energy transfer behavior of DIS [19,20]. However, it is not clear why duality should also work in a localized region, and even at relatively low momentum transfers.

Inclusive deep inelastic scattering on nucleons is a firmly-established tool for the investigation of the quark-parton model. At large enough values of W^2 and Q^2 , with $W^2 \gg Q^2$, a precise description of the Q^2 behavior of the nucleon structure function $F_2 = \nu W_2$ can be given in terms of a perturbative series in $\alpha_S(Q^2)$, up to NLO [21,22]. Such Q^2 behavior becomes especially transparent in comparing the high Q^2 (> 10 (GeV/c) 2) moments of F_2 with pQCD predictions [20,6].

An analysis of the resonance region at smaller W^2 and Q^2 in terms of QCD was first presented in Refs. [10], where Bloom and Gilman’s duality was re-interpreted: The integrals of the structure function, performed in [15] over the energy transfer ν , were translated into integrals over the variable x (or Nachtmann $\xi = 2x/(1 + \sqrt{1 + 4M^2x^2/Q^2})$ [23], in order to account for finite target mass effects). Bloom-Gilman duality was translated

into a correspondence between the $n=2$ moment of the F_2 structure function in the low Q^2 region, characterized by resonances, and in the high Q^2 scaling region, respectively. The fall of the resonances along a smooth scaling curve with increasing Q^2 was to be attributed [10] to the fact that there exist only small changes in the low n moments of the F_2 structure function due to power corrections in addition to the predicted perturbative ones. The appearance of power corrections is interpreted as a signal of deviations of the inclusive cross section from perturbative predictions, which one can envisage as due to the increasing importance of interactions between the quark struck in the electron-nucleon hard scattering process and the other quarks in the nucleon. In inclusive DIS, the Operator Product Expansion applies and power corrections are determined by the matrix elements of operators of higher twist (dimension-spin), which are related to multiparton configurations.

Such effects are inversely proportional to Q^2 , and can therefore be large at small Q^2 . If they are not, averages of the F_2 structure function over a sufficient range in x at moderate Q^2 are approximately the same as at high Q^2 . Notwithstanding, the dynamical origin of local duality, and thus the reason why the higher-twist contributions, undoubtedly required to construct the coherent nucleon resonances, tend to largely cancel on average, even at momentum transfers below 5 (GeV/c) 2 , is still not understood [6,8].

III. LOCAL DUALITY AT LOW MOMENTUM TRANSFER

In Fig. 1 we show an overview of recent high-precision proton resonance F_2 data at low Q^2 [4]. We also include data from SLAC at $Q^2 < 0.3$ (GeV/c) 2 [5]. For the former, the systematic uncertainty is estimated to be 3.5% [4]. For the latter, due to uncertainties in absolute normalization and radiative corrections, we estimate the systematic uncertainty to be better than 10%. The solid curves represent, for the different kinematics, the single scaling curve defined by averaging *all* nucleon resonance F_2 data, regardless of Q^2, W^2 , as a function of ξ [4]. As one can see the individual spectra, at various Q^2 , oscillate around this single-curve parameterization. We emphasize that this is **not** by construction, as the parameterization, at any given value of ξ , is obtained from a range of nucleon resonance data at variant values of Q^2 and W^2 (e.g., the second resonance bump could have always been below the scaling curve, while the first above, etc.). Our main observation is that apparently nature forces the oscillatory behavior of the various resonance bumps around a scaling curve, which has a valence-like behavior.

This has been studied quantitatively in [4] where it was observed that the behavior of averaged nucleon res-

onance data at $\xi > 0.3$, corresponding to $Q^2 \geq 0.5$ (GeV/c)² in the nucleon resonance region, is indistinguishable from the F_2 DIS behavior, consistent with the findings of Bloom and Gilman [15]. The behavior of averaged nucleon resonance data for $\xi < 0.3$, corresponding to $Q^2 < 0.5$ (GeV/c)² in the nucleon resonance region, mimics [3] xF_3 data obtained from averaging neutrino and antineutrino DIS data [24]. The latter, to leading order in QCD, selects the difference of quark and antiquark distribution functions, and is predominantly sensitive to a valence quark only distribution.

Increasing from $Q^2 \approx 0.07$ (GeV/c)² (Fig. 1a) to $Q^2 \approx 3$ (GeV/c)² (Figs. 1h,1i) the F_2 spectra change shape drastically. The low Q^2 spectrum shows a predominant $N-\Delta$ transition (we do not show the elastic peak, huge at this Q^2), and relatively minor strength at larger energy transfers. This is not surprising, as at these relatively small energy and four-momentum transfers one would expect to predominantly excite the valence quarks. At $Q^2 = 3.0$ (GeV/c)², on the other hand, one sees that the prominent nucleon resonances are largely reduced, and the inelastic background enhanced. Furthermore, F_2 in the higher resonance regions is larger than F_2 in the $N-\Delta$ transition region. Apparently, a swap of strength has occurred between the various channels as a function of Q^2 .

To further illustrate how the nucleon resonances seem to follow a valence-like curve, we show in Fig. 2 the behavior of the $N-\Delta$ transition region (here defined as $1.2 < W^2 < 1.9$ GeV²) and the second resonance region (defined as $1.9 < W^2 < 2.5$ GeV²) for various Q^2 as a function of ξ , in comparison with the global scaling curve defined in [3], and used in Fig. 1. As concluded in Refs. [3,4], it seems that the nucleon resonances slide along one global scaling curve (note that the apparent difference in scaling curve between Figs. 1 and 2 reflects only the conversion from W^2 to ξ , for fixed Q^2). One can see that, if nature forces the oscillatory behavior around a global scaling curve even at low Q^2 , the resonance excitation strengths will necessarily grow in the region below $\xi \approx 0.25$ where the maximum of the global scaling curve occurs, and subsequently decrease once the maximum of the global scaling curve has been crossed. Compare, for instance, the behavior of the $N-\Delta$ transition region with that of the larger-mass resonance regions: at $Q^2 = 0.45$ (GeV/c)² (solid circles in Fig. 2 (top), and Fig. 1c) the $N-\Delta$ transition region strength is large being at about the maximum of the scaling curve. Its strength, as for all $Q^2 < 0.45$ (GeV/c)², is also larger than the higher-mass resonance regions which lie at lower ξ for the same Q^2 . On the other hand, for $Q^2 \approx 3.0$ (GeV/c)² (open circles in Fig. 2(top), and Fig. 1h) the $N-\Delta$ transition region strength is small because it is positioned at large ξ , and smaller than the higher-mass resonance regions that lie at lower values of ξ , but have crossed the maximum of the scaling curve. The smooth curve, to which the nucleon

resonance regions tend, determines the momentum transfer dependence of the various nucleon resonance regions, forcing the nucleon elastic and transition form factors to scale like Q^{-4} [25] at relatively small Q^2 , resembling the Q^{-4} scaling as predicted by QCD counting rules.

We now ask the question: Can the observed behavior of the averaged nucleon resonance spectra be explained within pQCD?

In Fig. 3, we show a compilation of the world's electron-proton scattering data for the F_2 structure function at low Q^2 . The deep inelastic ($W^2 > 4$ GeV²) data originate from SLAC [26], CERN (NMC) [27], FNAL (E665) [28], and DESY (H1,ZEUS) [29–33,11]. As before we include data in the proton resonance region from SLAC [5] and JLab [3]. The solid curves indicate the next-to-leading order parameterizations of Glück, Reya, and Vogt (GRV) [34,35], which use input parton distributions starting from very low Q^2 values. In the third panel down of Fig. 3, the GRV calculation is the GRV input distribution at $Q^2 = 0.4$ (GeV/c)² [35], without any evolution, *neglecting sea and gluon contributions*. As one can see, the proton resonance region data for $Q^2 = 3.1$ (GeV/c)² and $Q^2 = 0.9$ (GeV/c)² smoothly join the deep inelastic data, and agree well with the GRV next-to-leading order calculations, exhibiting the local duality witnessed by Bloom and Gilman [15].

Turning our attention to the bottom two panels of Fig. 3, the low Q^2 F_2 data, we are only left with the recent DESY data [32,33], some sparse FNAL data [28], and the nucleon resonance data [5,3]. The DESY data exhibit the well-known collapse of the proton structure functions at (very) small x . One interpretation of this effect is that, at these small Q^2 , one sees a smooth transition from DIS to the real photon point at $Q^2 = 0$ [33,11,36]. Gauge invariance requires that, for consistency near $Q^2 = 0$, the structure function F_2 for inelastic channels must vanish like $Q^2\sigma(\gamma p)/(4\pi^2\alpha_{em})$ [36].

We emphasize here the difference in reaching the low Q^2 region for the various values of x . In Fig. 4 we distinguish among three different limits (indicated by the three arrows in the figure). For the DESY experiments, low Q^2 is established at small x by having a large (\approx constant) amount of energy transfer ν . For this reason, it is expected that this region exhibits similar characteristics as the parton model. For the JLab/SLAC experiments at $x \approx 0.1$, one reaches low Q^2 at relatively small energy transfers. If the limit is taken at *fixed* x , $x \approx 0.1$, the resonance data do not exhibit such a drastic collapse with Q^2 as observed at HERA, and they stay fairly constant. In fact, they still seem to oscillate around one Q^2 -independent global curve [3], informing us that the Q^2 dependence of the larger x nucleon resonance data is rather shallow. It is this behavior that makes the scaling curve of Figs. [1,2], defined by the world's nucleon resonance F_2 data, look “valence-like” [3]. If, instead, one takes the limit at a fixed W^2 , by restricting oneself

always to the nucleon resonance region ($M^2 < W^2 \leq 4 \text{ GeV}^2$), then one can see that the nucleon resonances “slide” down the x scale to lower x for lower Q^2 (*e.g.* see the constant $W = 2 \text{ GeV}$ arrow in Fig. 4), where their strength dies out as a function of Q^2 .

IV. MOMENTS OF F_2^P

We construct the experimental moments of the structure function, F_2 , for the Q^2 range up to 10 $(\text{GeV}/c)^2$. The Cornwall-Norton moments are defined as

$$M_n(Q^2) = \int_0^{x_{thr}} dx x^{n-2} F_2(x, Q^2), \quad (1)$$

and the Nachtmann moments as

$$M_n(Q^2) = \int_0^{x_{thr}} dx \frac{\xi^{n+1}}{x^3} \left[\frac{3 + 3(n+1)r + n(n+2)r^2}{(n+2)(n+3)} \right] \nu W_2(x, Q^2). \quad (2)$$

Here, $r = (1 + 4M^2 x^2 / Q^2)^{1/2}$, and x_{thr} is Bjorken x for pion threshold. We add to these integrals the elastic contribution, at $x = 1$, where

$$\nu W_2(x, Q^2) = \delta(1-x) \frac{\left(G_E^2(Q^2) + \frac{Q^2}{4M^2} G_M^2(Q^2) \right)}{\left(1 + \frac{Q^2}{4M^2} \right)}. \quad (3)$$

G_E (G_M) is the proton electric (magnetic) form factor. For the proton form factors, we use a fit to the world’s data by Bosted [37].

To obtain the inelastic contributions, we integrate data like those shown in Figs. 1 and 3. Apart from the data shown in Fig. 1, we have added Q^2 points where additional data were available. For $Q^2 < 0.6 \text{ (GeV}/c)^2$, we have constrained our search to elastic and nucleon resonance data. For $0.6 < Q^2 < 4 \text{ (GeV}/c)^2$, we have used nucleon resonance data in combination with deep inelastic data, whereas for $Q^2 > 4 \text{ (GeV}/c)^2$ we have constructed the moments utilizing both deep inelastic and nucleon resonance models, similar as in Ref. [9]. For the smallest values of Q^2 ($< 0.6 \text{ (GeV}/c)^2$), we assume a constant value of F_2 below x for $W^2 = 4.0 \text{ GeV}^2$, as only sparse data exists. As one can see from Fig. 3, this may not be a bad approximation for $Q^2 < 0.6 \text{ (GeV}/c)^2$, especially since the nucleon resonance region data extend down to $x \leq 0.1$, and the integration area below $x = 0.1$ is expected to be small only. To judge the uncertainty in this procedure, we have also integrated the $Q^2 \approx 0.2 \text{ (GeV}/c)^2$ data starting at $W^2 = 9.0 \text{ GeV}^2$ (rather than $W^2 = 4.0 \text{ GeV}^2$). This changes the second moment by less than 3%. Lastly, in some cases, we used a model to construct data at fixed Q^2 , rather than allowing for the

small range of Q^2 in the data. This effect on the second moments was found to be small, $< 3\%$, and far smaller for the higher moments. Thus, we believe the total uncertainty in the moments we calculate to be less than 5%. We show the values for the second, fourth, sixth, and eighth Cornwall-Norton (top) and Nachtmann (bottom) moments of the proton, extracted from the world’s data, including deep inelastic, nucleon resonance, and elastic data, as described above, in Fig. 5. Similarly, Tables I and II list the numerical values of the moments, with the elastic contribution to each separately given.

As expected, the elastic contribution dominates the moments at the lowest Q^2 . Note that the Cornwall-Norton moments will become unity, *i.e.* the proton charge squared, at $Q^2 = 0$, whereas the Nachtmann moments will vanish at $Q^2 = 0$, as can readily be seen from Eqn. 3. This can be attributed to the fact that, with respect to Bjorken x , the Nachtmann scaling variable ξ correctly takes into account the finite proton mass scale [23], but does not account for any other significant mass scale (like the quark masses). As the interpretation of the Cornwall-Norton moments in the $Q^2 < 1 \text{ (GeV}/c)^2$ region seems more intuitive, and we are interested here in the low- Q^2 behavior of the moments, we will concentrate on these moments in the remainder of the discussions in this work. To emphasize that there is indeed not much difference between the Cornwall-Norton and Nachtmann moments if one concentrates on the low- Q^2 region where the elastic contribution turns dominant, Fig. 6 graphically displays the relative contribution of the elastic channel to the total moment for both Cornwall-Norton (top) and Nachtmann (bottom) moments, for $n = 2$ (solid circles), $n = 4$ (squares), $n = 6$ (triangles) and $n = 8$ (stars), from Tables I and II. Nonetheless, as the benefit of the Nachtmann moments is to push an analysis in terms of an Operator-Product Expansion to lower values of Q^2 , taking correctly target-mass effects into account, we show everywhere similar figures, for comparison, for the Nachtmann moments. Note that one can argue that the relative contribution of the elastic grows slower for $Q^2 \rightarrow 0$ if one uses the Nachtmann moments.

First, let us revisit the large Q^2 , $Q^2 > 10 \text{ (GeV}/c)^2$, behavior of the moments. At asymptotically large Q^2 , one can write the non-singlet moments $M_n^{NS}(Q^2)$ at Leading Order (LO) ¹ in the perturbative expansion, as [22,6]

$$M_n^{NS}(Q^2) = A_n (\ln(Q^2/\Lambda^2))^{-1/d_n^{NS}}, \quad (4)$$

where Λ is the QCD scale parameter and

$$d_n^{NS} = \gamma_{o,n}^{NS} / 2\beta_o, \quad (5)$$

¹NLO corrections are important in general and will be discussed in detail in [38]. Their discussion is, however, not essential for discussing the points raised in the present paper.

where $\beta_o = 11 - (2/3)N_f$, with N_f the number of flavors, and $\gamma_{o,n}^{NS}$ the leading-order non-singlet anomalous dimensions numerically specified in [22]. To circumvent the requirement of non-singlet moments we highlight in Fig. 7 the $n = 4$ moment: although we use the same F_2 structure function data for all moments, the weighting with x^{n-2} in these moments will emphasize the large- x region, at higher n , and thus approximate a non-singlet moment. On the top of Fig. 7 we show the Cornwall-Norton moment, on the bottom the Nachtmann moment (each to the power $-1/d_n^{NS}$). We show the data in a log-log plot, in order to encompass also the low- Q^2 region. The moments are shown both with (stars) and without (open circles) the elastic contribution included.

The dashed curves exhibit a fit to the data, from [9], limited to $Q^2 > 20$ (GeV/c)² to minimize the effect of higher order corrections, in the form $[M_n^{NS}]^{(-1/d_n^{NS})} \approx P_1 \ln(Q^2/\Lambda^2)$. In [9], this fit gives $P_1 = 27.46$ (27.05) \pm 0.25 (0.24) and $\Lambda = 250$ MeV, for the Cornwall-Norton (Nachtmann) moment, rendering the expected logarithmic scaling behavior in QCD at asymptotic Q^2 . The dot-dashed (dotted) curves exhibit a similar fit in the form $(P_1 + P_2/Q^2 + P_3/Q^4)^{-1/d_n} \ln(Q^2/\Lambda^2)$ down to $Q^2 = 2.0$ (GeV/c)² from the same Reference [9], thus taking into account power corrections of order $1/Q^2$ and $1/Q^4$ ($1/Q^2$ only). Numerical values for the $1/Q^2$ and $1/Q^4$ coefficients are $P_2 = 0.33 \pm 0.04$ (0.33 ± 0.04) and $P_3 = 4.69 \pm 0.19$ (1.61 ± 0.15) for the Cornwall-Norton (Nachtmann) moment (see also the caption of Fig. 7). One can easily verify from Fig. 7 that the magnitude of the P_3 coefficient is in this case dominated by the inclusion of the elastic contribution. Similarly, the Nachtmann ($n = 4$) moment analysis gives a drastically different value for P_3 from the Cornwall-Norton ($n = 4$) moment analysis mainly due to the different contribution from the elastic.

In order to illustrate the relative strength of the elastic contribution compared to other W^2 regions, we show in Fig. 8 the second (Fig. 8a), fourth (8b), sixth (8c) and eighth (8d) Cornwall-Norton moments for $Q^2 < 5$ (GeV/c)², separated in the elastic contribution (squares, due to our choice of vertical scale sometimes only visible at the higher Q^2), the contribution of the $N - \Delta$ transition region (triangles, $1.2 < W^2 < 1.9$ GeV²), of the second resonance region (open circles, $1.9 < W^2 < 2.5$ GeV²) and of the “deep inelastic” region (stars, $W^2 > 4$ GeV²). The total moment is given by the solid circles, and the curves connect the various data to guide the eye. The chosen finite W^2 regions will start contributing to the moments at low Q^2 , recovering part of the loss of strength due to the fall-off of the elastic contribution, and then also die off, as the resonances move to the larger ξ side of the scaling curve. The contribution of the $W^2 > 4$ GeV² region does not die off, as this is not a finite W^2 region, so higher- W^2 resonances and/or higher- W^2 inelastic background start becoming important with in-

creasing Q^2 , eventually yielding the logarithmic behavior of the moments prescribed by QCD. As evidenced by the difference between the $W^2 > 4$ GeV² contribution and the total moment, the contribution of the region of $W^2 < 4$ GeV² is non-negligible up to $Q^2 \approx 5$ (GeV/c)², even for the second moment. Similar remarks hold for the various Nachtmann moments, shown in Fig. 9.

We note here also that the behavior of the second Cornwall-Norton F_2 moment we extract is very similar to the behavior in the second moment of the spin-dependent g_1 structure function [39]. Presently we only have sparse g_1 data in the nucleon resonance region, for $0.1 < Q^2 < 5$ (GeV/c)², such that we can not verify precisely whether the spin-dependent nucleon resonance data tend to oscillate around a similar smooth curve. However, the limited data are not inconsistent with such a behavior [40]. Also, we presently do not have enough data for the longitudinal structure function F_L to verify a similar onset of duality [41], although sparse hints do exist in the present world’s data [42].

V. DISCUSSION OF RESULTS

Our findings, that the moments of F_2 show a smooth transition from DIS down to $Q^2 \approx 0$ (GeV/c)², and that the nucleon resonances tend to oscillate around one smooth curve, support the findings of Ref. [43,44,38] that higher-twist effects are small if one looks at the low- Q^2 behavior of F_2 for $Q^2 \simeq 1$ (GeV/c)². The dynamical process of local duality dictates minimal Q^2 dependence of F_2 at small Q^2 ; in terms of pQCD this can be explained if the higher-twist effects are reduced *on average* in the nucleon resonance region [45]. Nonetheless, higher-twist effects must be responsible for the nucleon resonances themselves. The results for the lower moments of F_2 , presented here, show a forced transition from the elastic point to the large Q^2 limit, supported by the oscillations of the nucleon resonance region around one smooth curve at low Q^2 . This smooth curve resembles the deep inelastic data at $Q^2 \simeq 1$ (GeV/c)², and higher-twist effects continue to be small from there on.

The extension of a pQCD analysis to very low values of Q^2 , *i.e.* $Q^2 \rightarrow \Lambda^2$, is of doubtful predictivity. Here even the low n moments are mainly sensitive to the inclusion of the elastic contribution (as this contributes already close to 10% to the $n = 2$ moment at $Q^2 = 2$ (GeV/c)²): a picture in terms of non-interacting quark and gluon degrees of freedom is clearly no longer tenable. Similarly the most plausible interpretation of the behavior observed for the dynamical power corrections, which should represent the initial signature of NP effects overshadowing the perturbative expansion, would in fact be that their contribution in the $1/Q^2$ expansion is enhanced at decreasing values of Q^2 . However, this contribution can be damped on average if coefficients of different powers are large but with

opposite signs, thus causing the cancellation required to make the moment a slowly varying function of Q^2 only. These cancellations are evidently of NP origin and are at low Q^2 not easily associated to partonic degrees of freedom in the multiparton correlations.

One has to be careful making further concrete statements. E.g., it is often remarked that duality obviously does not work universally, as the $n = 2$ Cornwall-Norton moment at $Q^2 \rightarrow 0$ equals the coherent sum of the quark charges squared, which can not equal the parton model expectation in the Bjorken limit. First of all, F_2 is not purely transverse, which casts doubt on drawing too definite a conclusion at low values of Q^2 . Results of an experiment to measure $R = \sigma_L/\sigma_T$ in the nucleon resonance region are needed and forthcoming [46]. More importantly, the moment analysis will at lower and lower Q^2 be sensitive to a smaller and smaller region in ξ , as the inelastic region and nucleon resonances move to lower ξ and their absolute contribution to the moments diminishes. Even in a world without elastic electron-proton scattering, one would, at the lowest Q^2 , be mainly sensitive to a single resonance transition region, in this case the $N - \Delta$ transition region. This is illustrated in Fig. 10, where we repeat Fig. 5 for a world without elastic electron-proton scattering. It can easily be seen (Figs. 1, 3, 8, and 9) that the $N - \Delta$ transition contribution, defined by the region $1.2 < W^2 < 1.9 \text{ GeV}^2$, becomes more and more dominant at low Q^2 . Thus, in this world a moment analysis at low Q^2 would become dominated by the coherent $N - \Delta$ process. Still, *on average* the $N - \Delta$ transition region seems to obey duality, in that it oscillates around a similar smooth scaling curve. This is not inconsistent with the findings of [10], the discrete resonance transitions are reminiscent of large higher-twist effects, but on average still seem to cancel to large extent (although quantitatively perhaps not as well as at higher Q^2). The above example is not dissimilar to stating that duality will not work on top of any given resonance peak. A region over which to average is always required.

Furthermore, if one neglects the elastic channel, one will at low Q^2 be mainly sensitive to the imposed constraint by gauge invariance that the structure function F_2 must behave like $Q^2\sigma(\gamma p)/(4\pi^2\alpha_{em})$ [36]. At the values of x where the nucleon resonances are visible at low Q^2 in Fig. 3 (e.g. $x \approx 0.1$), the F_2 structure function does **not** linearly vanish with Q^2 yet, as shown in [3]. Thus, although the F_2 strength in the nucleon resonance region has to disappear linearly with Q^2 below some Q_0^2 , one can argue that the behavior of the data is not reflecting this $Q^2 < Q_0^2$ expectation yet. This indicates that the oscillations the nucleon resonances exhibit around a smooth curve, even down to $Q^2 \approx 0.1 \text{ (GeV/c)}^2$, is non-trivial. As the low- Q^2 F_2 data below $W^2 = 4 \text{ GeV}^2$ predominantly consists of excited nucleon resonances and hardly contributions from inelastic non-resonant processes, one can argue that such a smooth curve must be close to a

curve consisting of valence strength only. In fact, the Q^2 dependence of the integrated valence quark strength in the GRV model [34,35] is close to the Q^2 dependence of the second Cornwall-Norton moment of F_2 . However, this Q^2 dependence is predominantly due to the inclusion of the elastic channel. Thus, for a picture such as the GRV model to be valid, there must be a separate Q^2 dependence for the vanishing of the large- x strength at small Q^2 (governed by the nucleon resonances) and the growth of the small- x sea.

Such ideas are very similar as to what has been observed in hadron-hadron scattering [17]. Here, a generalization of the duality picture was introduced, in which resonances were dual to non-diffractive Regge pole exchanges, with the non-resonant contributions dual to Pomeron exchange. Within QCD, this corresponds to a picture where resonances are dual to valence quarks, while the non-resonant background is dual to sea quarks. This supports the importance of additional detailed studies of electron scattering in the nucleon resonance region, in a wide range of x and Q^2 .

VI. CONCLUSIONS

We show that the world's data on F_2 , down to $Q^2 \simeq 1 \text{ (GeV/c)}^2$, are reasonably well described within pQCD. This includes the nucleon resonance data, which average to an approximate scaling curve, due to local duality. Down to $Q^2 \simeq 0.1 \text{ (GeV/c)}^2$, the nucleon resonance data still tend to average to such a curve. The contribution of the nucleon resonances to the lower moments of F_2 dies out at very small Q^2 as they have moved to smaller Bjorken x . Instead, the moments below $Q^2 \approx 1 \text{ (GeV/c)}^2$ are dominated by the elastic contribution at large x . Therefore, a pQCD-based analysis of the low- Q^2 moments of F_2 will render coefficients of the higher-twist terms which are predominantly due to the elastic contribution. Local duality seems to hold down to at least $Q^2 \approx 0.5 \text{ (GeV/c)}^2$ and to prescribe the transition from the kinematic region dominated by the elastic contribution to the region dominated by deep inelastic scattering.

This work was supported in part by the U.S. Department of Energy under Grant No. DE-FG02-95ER40901, and the National Science Foundation under Grant No. HRD-9633750. The authors express gratitude to the Jefferson Lab Theory Group for many useful discussions. CEK acknowledges the support of an NSF Early Faculty Career Development Grant.

- [1] S. Catani *et al.*, Report of the “1999 CERN Workshop on SM Physics (and more) at the LHC”, S. Catani, M. Dittmar, D. Soper, W.J. Stirling, S. Tapprogge (convenors). CERN-TH/2000-131; hep-ph/0005025.
- [2] M. Beneke, Phys. Rep. **317** (1999) 1.
- [3] I. Niculescu *et al.*, Phys. Rev. Lett. **85** (2000) 1182.
- [4] I. Niculescu *et al.*, Phys. Rev. Lett. **85** (2000) 1186.
- [5] S. Stein *et al.*, Phys. Rev. D **12** (1975) 1884.
- [6] D.W. Duke and R.G. Roberts, Nucl. Phys. **B166** (1980) 243.
- [7] L.F. Abbott, W.B. Atwood and R. M. Barnett, Phys. Rev. D **22** (1980) 582.
- [8] X. Ji and P. Unrau, Phys. Rev. D **52** (1995) 73.
- [9] I. Niculescu, C. Keppel, S. Liuti, and G. Niculescu, Phys. Rev. D **60** (1999) 094001.
- [10] A. DeRujula, H. Georgi, and H.D. Politzer, Phys. Lett. **B64** (1976) 428; Annals of Phys. **103** (1977) 315.
- [11] J. Breitweg *et al.*, hep-ex/0005018 (2000).
- [12] Yu.L. Dokshitzer, Proceedings of the *29th International Conference on High-Energy Physics (ICHEP 98)*, Edited by A. Astbury, D. Axen, J. Robinson. Singapore, World Scientific, 1999, p.305; hep-ph/9812252.
- [13] P. Hoyer, “Talk given at 6th INT / Jlab Workshop on Exclusive and Semiexclusive Processes at High Momentum Transfer, Newport News, VA, 19-23 May 1999, hep-ph/9908501.
- [14] A.C. Mattingly and P.M. Stevenson, Phys. Rev. D **49** (1994) 437.
- [15] E.D. Bloom and F.J. Gilman, Phys. Rev. D **4** (1971) 2901; Phys. Rev. Lett. **25** (1970) 1140
- [16] L.D. Soloviev, A.A. Logunov, and A.N. Tavkhelidze, Phys. Lett. **B24** (1967) 181; K. Igi and S. Matsuda, Phys. Rev. Lett. **18** (1967) 625; R. Dolne, D. Horn, and C. Schmid, Phys. Rev. **166** (1968) 1768.
- [17] H. Harari, Phys. Rev. Lett. **20** (1968) 1395.
- [18] P.D.B. Collins, *An Introduction to Regge Theory and High Energy Physics* (Cambridge University Press, Cambridge, 1977)
- [19] F.E. Close, *An Introduction to Quarks and Partons* (Academic Press, Great Britain, 1979).
- [20] R. Roberts, *The Structure of the Proton* (Cambridge University Press, Cambridge, 1990)
- [21] G. Altarelli, Phys. Rep. **81** (1982) 1.
- [22] A.J. Buras, Rev. Mod. Phys. **52** (1980) 199.
- [23] O. Nachtmann, Nucl. Phys. **B63** (1975) 237.
- [24] J.M. Conrad, M.H. Shaevitz, and T. Bolton, Rev. Mod. Phys. **70** (1998) 1341.
- [25] P. Stoler, Phys. Rep. **226** (1993) 103.
- [26] L.W. Whitlow *et al.*, Phys. Lett. **B250** (1990) 193; L.W. Whitlow, Ph.D. Thesis, American University (1990); L. Tao *et al.*, Z. Phys. **C70**, 387 (1996);
- [27] M. Arneodo *et al.*, Nucl. Phys. **B483** (1997) 3.
- [28] M.R. Adams *et al.*, Phys. Rev. D **54** (1996) 3006.
- [29] S. Aid *et al.*, Nucl. Phys. **B470** (1996) 3.
- [30] M. Derrick *et al.*, Z. Phys. **C65** (1995) 379; *ibid.* **C69** (1995) 607.
- [31] M. Derrick *et al.*, Z. Phys. **C72** (1996) 399.
- [32] J. Breitweg *et al.*, Phys. Lett. **B407** (1997) 432.
- [33] J. Breitweg *et al.*, hep-ex/9809005 (1998).
- [34] M. Glück, E. Reya, and A. Vogt, Z. Phys. **C67** (1995) 433.
- [35] M. Glück, E. Reya, and A. Vogt, Eur. Phys. J. **C5** (1998) 461.
- [36] A. Donnachie and P.V. Landshoff, Z. Phys. **C61** (1994) 139.
- [37] P.E. Bosted, Phys. Rev. C **51** (1995) 409.
- [38] S. Liuti, *Talk presented at the Workshop on Nucleon Structure in High x-Bjorken Region (HiX2000), Philadelphia, Pennsylvania, 30 Mar - 1 Apr 2000.*; S. Liuti *et al.*, *in preparation.*
- [39] X. Ji and W. Melnitchouk, Phys. Rev. D **56** (1997) 1.
- [40] K. Abe *et al.*, Phys. Rev. D **58** (1998) 112003.
- [41] C. Carlson and N. Mukhopadhyay, Phys. Rev. D **41** (1990) 2343.
- [42] R. Ent, C.E. Keppel, and I. Niculescu, Phys. Rev. D **62** (2000) 73008.
- [43] U.K. Yang and A. Bodek, Phys. Rev. Lett. **82** (1999) 2467.
- [44] S.I. Alekhin and A.L. Kataev, Nucl. Phys. **A666-667** (2000) 179, *and references therein.*
- [45] H. Georgi and H.D. Politzer, Phys. Rev. D **14** (1976) 1829.
- [46] Jefferson Lab experiment E94-110, analysis in progress.

TABLE I. Cornwall-Norton Moments for $n = 2, 4, 6$, and 8 at $0.15 \leq Q^2 \leq 4.3$ (GeV/c) 2 , as extracted from the data (see text). The elastic contribution is given as a separate column. The uncertainties of the total moments are smaller than 5%.

Q^2 (GeV/c) 2	elastic	$n = 2$	$n = 4$	$n = 6$	$n = 8$
0.15	0.592	0.652	0.594	0.592	0.592
0.20	0.504	0.584	0.508	0.505	0.504
0.45	0.249	0.379	0.261	0.251	0.250
0.55	0.195	0.341	0.210	0.198	0.196
0.85	0.103	0.278	0.122	0.107	0.104
0.94	0.087	0.264	0.107	0.092	0.088
1.40	0.040	0.231	0.064	0.047	0.043
1.70	0.026	0.219	0.051	0.034	0.029
2.40	0.011	0.203	0.036	0.019	0.014
3.00	0.006	0.196	0.030	0.013	0.009
3.30	0.005	0.192	0.028	0.012	0.008
4.30	0.002	0.184	0.023	0.008	0.005

TABLE II. Nachtmann Moments for $n = 2, 4, 6$, and 8 at $0.15 \leq Q^2 \leq 4.3$ (GeV/c) 2 , as extracted from the data (see text). The elastic contributions, different for each n , are given as a separate entity in the columns. The uncertainties of the total moments are smaller than 5%, and the numbers quoted can be used to this precision.

Q^2	$n = 2$		$n = 4$		$n = 6$		$n = 8$	
	elas.	total	elas.	total	elas.	total	elas.	total
0.15	0.274	0.333	0.040	0.041	0.0051	0.0052	0.0006	0.0006
0.20	0.256	0.322	0.047	0.049	0.0074	0.0075	0.0011	0.0011
0.45	0.160	0.281	0.050	0.057	0.0139	0.0146	0.0037	0.0038
0.55	0.131	0.268	0.046	0.056	0.0146	0.0157	0.0045	0.0046
0.85	0.076	0.243	0.034	0.047	0.0137	0.0157	0.0054	0.0057
0.94	0.065	0.235	0.030	0.045	0.0130	0.0154	0.0054	0.0058
1.40	0.032	0.217	0.018	0.036	0.0093	0.0128	0.0047	0.0055
1.70	0.022	0.209	0.013	0.033	0.0073	0.0114	0.0040	0.0051
2.40	0.010	0.197	0.007	0.027	0.0041	0.0089	0.0026	0.0040
3.00	0.005	0.192	0.004	0.024	0.0026	0.0075	0.0018	0.0033
3.30	0.004	0.189	0.003	0.023	0.0021	0.0071	0.0015	0.0031
4.30	0.002	0.181	0.001	0.020	0.0011	0.0058	0.0008	0.0024

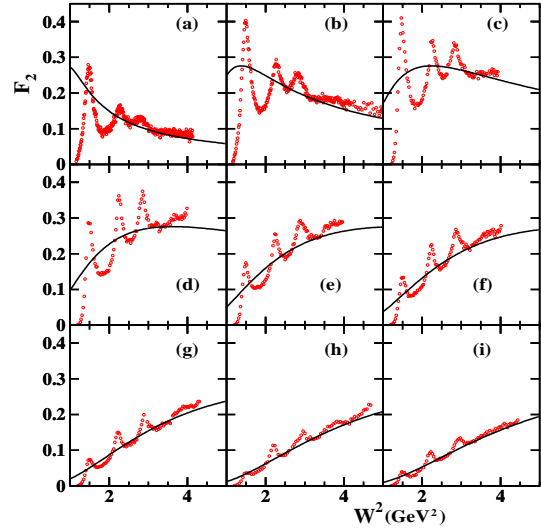


FIG. 1. F_2 Spectrum in the nucleon resonance region as a function of W^2 , for values of $Q^2 = 0.07$ (a), 0.20 (b), 0.45 (c), 0.85 (d), 1.40 (e), 1.70 (f), 2.40 (g), 3.00 (h) and 3.30 (i) (GeV/c) 2 . We have superimposed the results from the scaling curve from Ref. [4], to illustrate the behavior of the nucleon resonance region with increasing Q^2 .

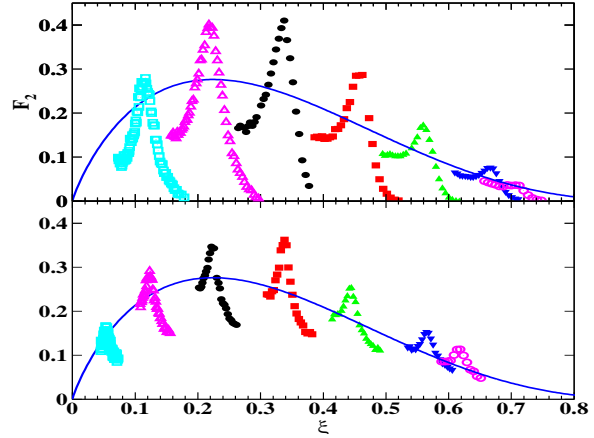


FIG. 2. F_2 data for the regions $1.2 < W^2 < 1.9$ (top) and $1.9 < W^2 < 2.5$ (bottom) GeV 2 , as a function of Nachtmann ξ . Data are shown for $Q^2 = 0.07, 0.20, 0.45, 0.85, 1.4, 2.4$, and 3.0 (GeV/c) 2 (left to right), respectively. The solid curve represents the scaling curve, determined by averaging *all* nucleon resonance data [4].

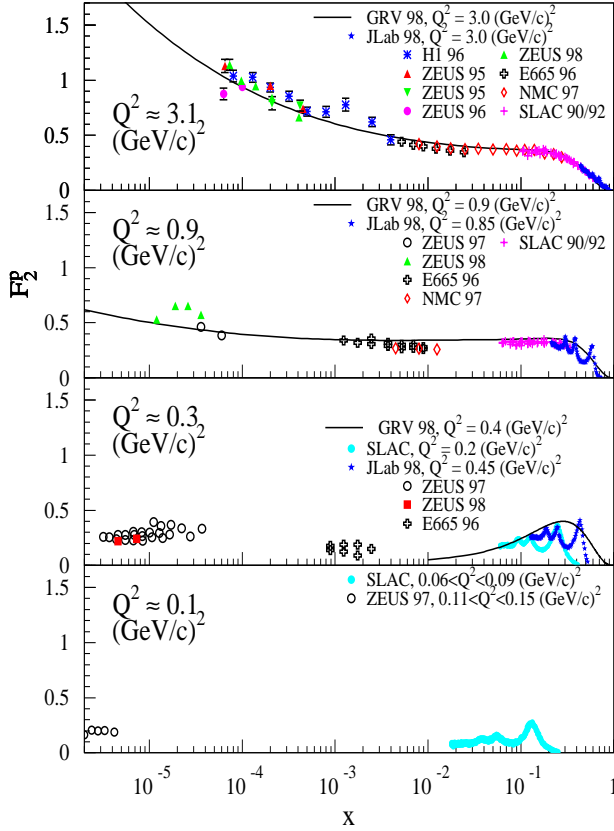


FIG. 3. F_2 as a function of x for four values of Q^2 , with a logarithmic x scale. The symbols indicate various experiments, as cited in the text. The solid curves in the top two panels represent the calculated distributions from the GRV collaboration [34,35], evolved from $Q^2 = 0.4$ (GeV/c) 2 . The solid curve in the third panel represents the input distribution itself.

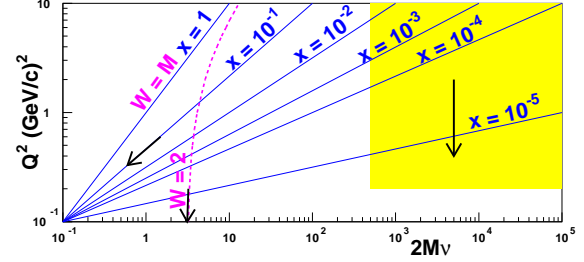


FIG. 4. Kinematics region of the world's F_2 structure function data, for $Q^2 < 10$ (GeV/c) 2 . Thin lines are for fixed Bjorken x . The dashed line is for fixed $W = 2$ GeV, indicating the border of the region typically associated with the nucleon resonances (the other border being fixed $W = M$, or $x = 1$). The shaded area exhibits the kinematics region of the recent DESY measurements [29–33]. The thick arrows indicate various manners in which one can reach the limit $Q^2 \rightarrow 0$, at fixed x , fixed W , or fixed ν .

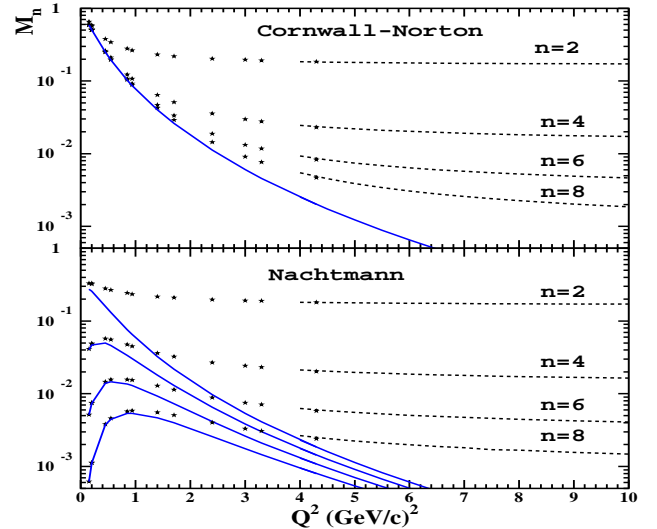


FIG. 5. Cornwall-Norton moments (top) and Nachtmann moments (bottom) extracted from the world's electron-proton scattering data, for $n = 2, 4, 6$, and 8 . The solid lines indicate the elastic contribution. At low Q^2 (≤ 4.3 (GeV/c) 2) the moments (stars) are directly constructed from the world's electron-proton F_2 database (see text). At larger Q^2 , the moments have been extracted from appropriate fits to the world's data on inclusive scattering to both the nucleon resonance and deep inelastic regions (dashed lines) [9].

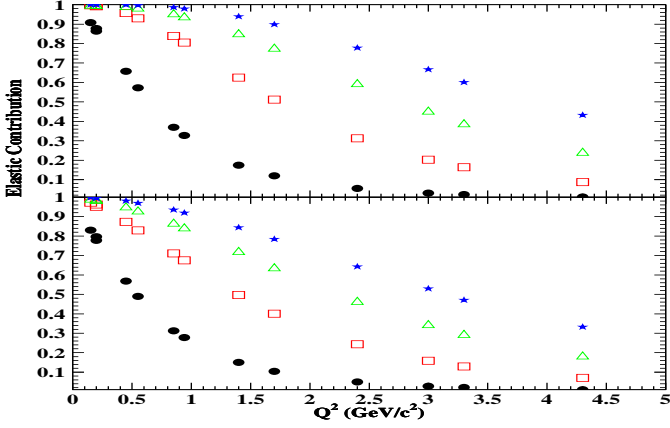


FIG. 6. Contribution of the elastic channel to the Cornwall-Norton moments (top) and Nachtmann moments (bottom) extracted from the world's electron-proton scattering data, for $n = 2$ (solid circles), 4 (squares), 6 (triangles), and 8 (stars), up to $Q^2 = 5$ (GeV/c)². The data are from Tables I and II.

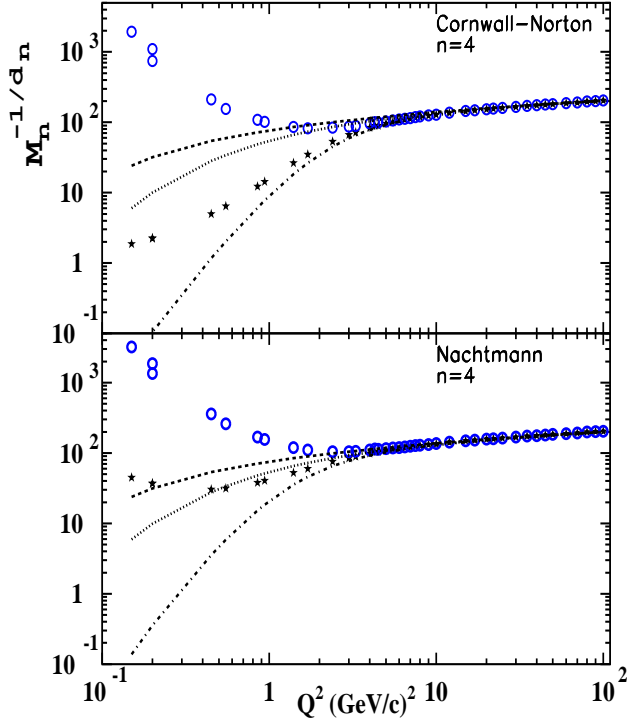


FIG. 7. Log-log plot of the $n = 4$ Cornwall-Norton (top) and Nachtmann (bottom) $M_n(Q^2)^{-1/d_n}$ moment as a function of Q^2 , where $d_n = \gamma_0^n / 2\beta_0$ [20]. Stars (open circles) do (do not) include the elastic contribution. In the top plot, the dashed curve is a fit to the $n = 4$ moment in the form $P_1 \ln(Q^2/\Lambda^2)$, from [9], with $P_1 = 27.46 (\pm 0.25)$, and $\Lambda = 250$ MeV. Similarly, the dotted curve uses a form $(P_1 + P_2/Q^2) \ln(Q^2/\Lambda^2)$, with $P_2 = 0.33 (\pm 0.04)$, and the dot-dashed curve uses a form $(P_1 + P_2/Q^2 + P_3/Q^4) \ln(Q^2/\Lambda^2)$, with $P_3 = 4.69 (\pm 0.19)$. In the bottom plot, the fit parameters are $P_1 = 27.05 (\pm 0.24)$, $P_2 = 0.33 (\pm 0.04)$, and $P_3 = 1.61 (\pm 0.15)$, respectively [9].

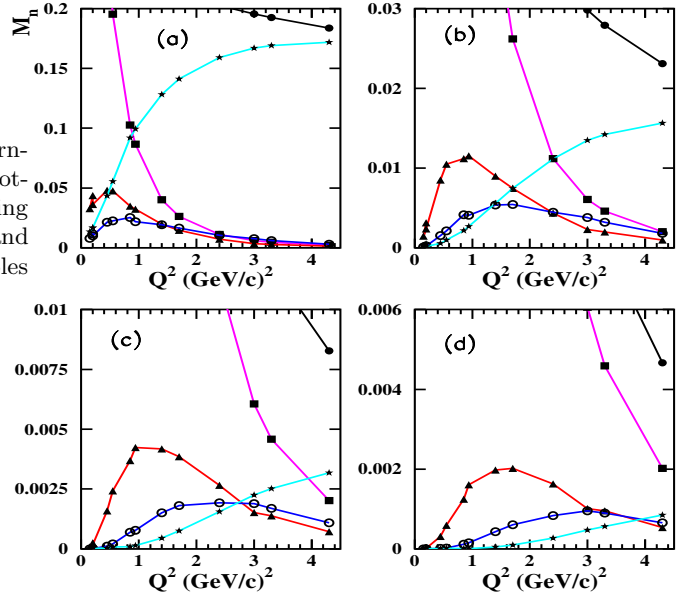


FIG. 8. Second (a), fourth (b), sixth (c) and eighth (d) Cornwall-Norton moments. Contributions due to the elastic peak (squares), the regions $1.2 < W^2 < 1.9$ GeV² (triangles), $1.9 < W^2 < 2.5$ GeV² (open circles), and $W^2 > 4$ GeV² (stars) are separately shown, in combination with the total moment (solid circles), as a function of the momentum transfer. Curves connect the various data, and are to guide the eye only.

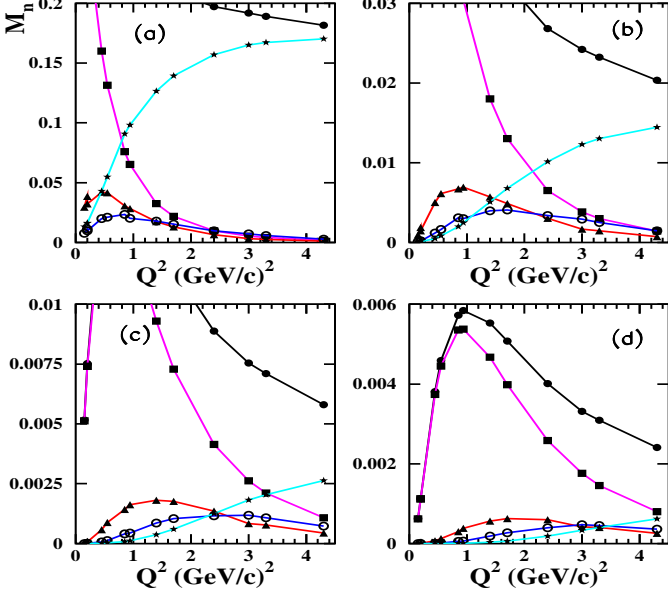


FIG. 9. Second (a), fourth (b), sixth (c) and eighth (d) Nachtmann moments. Contributions due to the elastic peak (squares), the regions $1.2 < W^2 < 1.9 \text{ GeV}^2$ (triangles), $1.9 < W^2 < 2.5 \text{ GeV}^2$ (open circles), and $W^2 > 4 \text{ GeV}^2$ (stars) are separately shown, in combination with the total moment (solid circles), as a function of the momentum transfer. Curves connect the various data, and are to guide the eye only.

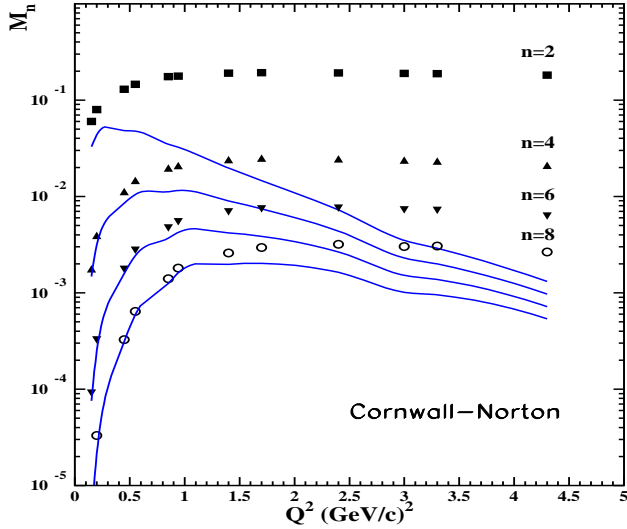


FIG. 10. Cornwall-Norton moments extracted from the world's electron-proton scattering data, for $n = 2, 4, 6$, and 8 , **without the elastic contribution included**. The solid lines connect the calculated contributions from the $N - \Delta$ transition region ($1.2 < W^2 < 1.9 \text{ GeV}^2$) at various Q^2 .